

# A facile strategy to integrate robust porous aluminum foil into microfluidic chip for sorting particles

Yi-Shan Zeng<sup>2</sup> · Hua Fan<sup>2</sup> · Bing Xu<sup>1</sup> · Zhen Zhang<sup>1</sup> · Fei-Fei Ren<sup>3</sup> · Chen Zhou<sup>4</sup> · Si-Zhu Wu<sup>4</sup> · Yan-Lei Hu<sup>1</sup> · Wu-Lin Zhu<sup>1</sup> · Ya-Hui Su<sup>3</sup> · Jia-Ru Chu<sup>1</sup> · Jia-Wen Li<sup>1</sup> · Guo-Qiang Li<sup>1</sup> · Dong Wu<sup>1</sup>

Received: 14 February 2017 / Accepted: 26 September 2017 / Published online: 6 November 2017  
© Springer-Verlag GmbH Germany 2017

**Abstract** High efficiency integration of functional micro-devices into microchips is crucial for broad microfluidic applications. Here, a device-insertion and pressure sealing method was proposed to integrate robust porous aluminum foil into a microchannel for microchip functionalization which demonstrate the advantage of high efficient foil micro-fabrication and facile integration into the microfluidic chip. The porous aluminum foil with large area ( $10 \times 10 \text{ mm}^2$ ) was realized by one-step femtosecond laser perforating technique within few minutes and its pores size could be precisely controlled from  $3 \mu\text{m}$  to millimeter scale by adjusting the laser pulse energy and pulse number. To verify the versatility and flexibility of this method, two kinds of different microchips were designed and fabricated. The vertical-sieve

3D microfluidic chip can separate silicon dioxide ( $\text{SiO}_2$ ) microspheres of two different sizes (20 and  $5 \mu\text{m}$ ), whereas the complex stacking multilayered structures (sandwich-like) microfluidic chip can be used to sort three different kinds of  $\text{SiO}_2$  particles (20, 10 and  $5 \mu\text{m}$ ) with ultrahigh separation efficiency of more than 92%. Furthermore, these robust filters can be reused via cleaning by backflow (mild clogging) or disassembling (heavy clogging).

## 1 Introduction

In the past decades, microfluidic chip has attracted great attention due to its advantages of ultralow reagent consumption, low cost, high-speed, high integrity, portability and miniaturization (Whitesides 2006). For practical applications, a variety of functions such as pumping, mixing, trapping and sorting was integrated into microfluidic chip. Among them, separation is one of the most important functions for chemical and biological applications. The present separation methods can be classified into two categories: active techniques and passive techniques (Sajeesh and Sen 2014). The former one always requires external field such as magnetic (Kang and Park 2007; McCloskey et al. 2003; Weddemann et al. 2009), optical (MCGloin 2006; Dholaria and Cižmar 2011; Xiao and Grier 2010) and acoustic (Nilsson et al. 2004; Nam et al. 2012; Liu and Lim 2011; Shi et al. 2008) to control the interaction between particles, microchannel structures and the flow field. For the latter methods, such as pinched flow fractionation (Yamada et al. 2004; Jain and Posner 2008; Takagi et al. 2005) and inertia flow fractionation (Park and Jung 2009; Ali et al. 2008; Yoon et al. 2009), flow velocity need to be precisely controlled to achieve the separation.

**Electronic supplementary material** The online version of this article (doi:10.1007/s10404-017-2001-9) contains supplementary material, which is available to authorized users.

✉ Yan-Lei Hu  
huyl@ustc.edu.cn

✉ Dong Wu  
dongwu@ustc.edu.cn

<sup>1</sup> CAS Key Laboratory of Mechanical Behavior and Design of Materials, Department of Precision Machinery and Precision Instrumentation, University of Science and Technology of China, Hefei 230026, Anhui, People's Republic of China

<sup>2</sup> Department of Mechanical and Electronic Engineering, Hefei University of Technology, Hefei 230009, Anhui, People's Republic of China

<sup>3</sup> School of Electrical Engineering and Automation, Anhui University, Hefei 230601, Anhui, People's Republic of China

<sup>4</sup> School of Instrument Science and Opto-Electronics Engineering, Hefei University of Technology, Hefei 230009, Anhui, People's Republic of China

As a commonly passive technique, the size-based method (Sethu et al. 2006; Mohamed et al. 2007; Zheng et al. 2007) separates particles without any external field and velocity demand, which means it can be easily applied in a miniaturized chip for further research such as point-of-care diagnostic test. Various methods have been proposed to integrate the filtering membrane into a microchip for realizing the size-based separation. For example, femtosecond laser two-photon polymerization (TPP) microfabrication can directly fabricate regular multiporous membranes inside a microchannel, but the fabrication process is too complicated, time-consuming and not suitable for large-area fabrication (Wei et al. 2011; Xu et al. 2016). Moorthy and Beebe (2003) directly fabricated the porous filters by ‘emulsion photopolymerize’ in the pre-defined location of a channel. Xiao et al. (2010) used assembly and transfer printing method to fabricate and integrate the porous structure into microchannel. Although their methods are convenient, both of the pores size and position cannot be precisely tuned to fulfill the demands for sorting particles with different sizes. Wei et al. (2011) used soft lithography to fabricate the PDMS membrane and integrated it into a microfluidic chip by prepolymer bonding, whereas the multistep fabrication of the membrane is complex and difficult to operate. Moreover, the PDMS film (20  $\mu\text{m}$  thickness) is too soft and elastic which tends to collapse when endures with continuous flow. Besides, in order to realize the separation function, many packaging methods have been developed for integration of functional membranes into a microfluidic chip. Traditional packaging methods such as thermal bonding can directly bond multilayer structure (Aran et al. 2010; Wu and Steckl 2009), whereas the different thermal expansion coefficients of the individual layers may cause distortion of the porous membrane. The prepolymer which is employed to bond the microchip and membrane may block the channel and the membrane. In addition, these bonding methods are irreversible, which means the chip can only be used for one time.

Here, we present a device-insertion and pressure sealing technique for alternative particle separation, which involves a simple step of inserting robust porous metal aluminum foil (25  $\mu\text{m}$  thickness) into a microchannel for functional microchips. The microchip can separate particles of various sizes by simply substituting with appropriate aluminum foil using femtosecond laser perforating technique (Li et al. 2015a, b; Sugioka and Cheng 2014; Wang 2005; Jiang et al. 2016), which can fabricate porous foils with controllable micropores of sizes from 3  $\mu\text{m}$  to several mm (Supplementary Material) by adjusting the laser pulse energy and pulse number. The total time for creating of  $200 \times 200$  porous arrays ( $4.8 \times 4.8 \text{ mm}^2$ ) is less than 30 min. The robust aluminum foil shows strong mechanical strength and can be reused many times by ultrasound cleaning. The insertion and pressure sealing method is simple, rapid and effective

in contrast to other integrated methods as mentioned above. At last, a sandwiched-like microfluidic chip with integrating of two kinds of aluminum foil with different pores sizes is designed to sort three different kinds of particles (5, 10 and 20  $\mu\text{m}$  diameters) with high separation efficiency ( $> 92\%$ ). We believe this promising approach combining femtosecond laser perforating and easy packaging of a microfluidic chip can be widely applied in a variety of fields including particle purification, blood cells separation and cell-sample preparation.

## 2 Experimental

### 2.1 Material

Poly (dimethylsiloxane) (PDMS) was supplied by Dow Corning (USA). Silicon dioxide ( $\text{SiO}_2$ ) microspheres with diameters of 5, 10 and 20  $\mu\text{m}$  were manufactured by Huge Biotech Corp. (Shanghai, China). The aluminum foil was purchased from New Metal Material Tech. Corp. (Beijing, China). The glass used as the master for the sandwich structure was obtained from Citotest Corp. (Jiangsu, China). The stainless steel wire with 275  $\mu\text{m}$  diameter was purchased from a local store.

### 2.2 Fabrication of aluminum foil with micropore arrays

The porous aluminum foil as the filtering membrane was fabricated by a regenerative amplified Ti: sapphire femtosecond laser system (Legend Elite-1K-HE, Coherent, USA) which generates 104 fs pulses at a repetition rate of 1 kHz with a central wavelength of 800 nm. The diameters of the pores can be tuned from 3  $\mu\text{m}$  to several millimeters by adjusting the laser pulse energy and pulse number. The advantages of this technique are rapid and suitable for large-area fabrication. Details of the micropore aluminum foil processing were described in the Supplementary Material. A field-emission scanning electron microscope FE-SEM (JSM-6700F, JEOL, Tokyo, Japan) was utilized for the micropore characterization.

### 2.3 Fabrication of the vertical-sieve 3D microchip

The schematics of the insertion and pressure sealing technique are shown in Fig. 1a. Firstly, the microchannel with 275  $\mu\text{m}$  diameter was fabricated by using the stainless steel wire as the mold. A curing agent and the PDMS prepolymer mixed by 1:10 weight ratio were poured into a Petri dish where the stainless steel wire was fixed in the middle of it. The thickness of the PDMS was about 10 mm. After curing on a hotplate at 80  $^\circ\text{C}$  for 3 h, the PDMS slab was peeled

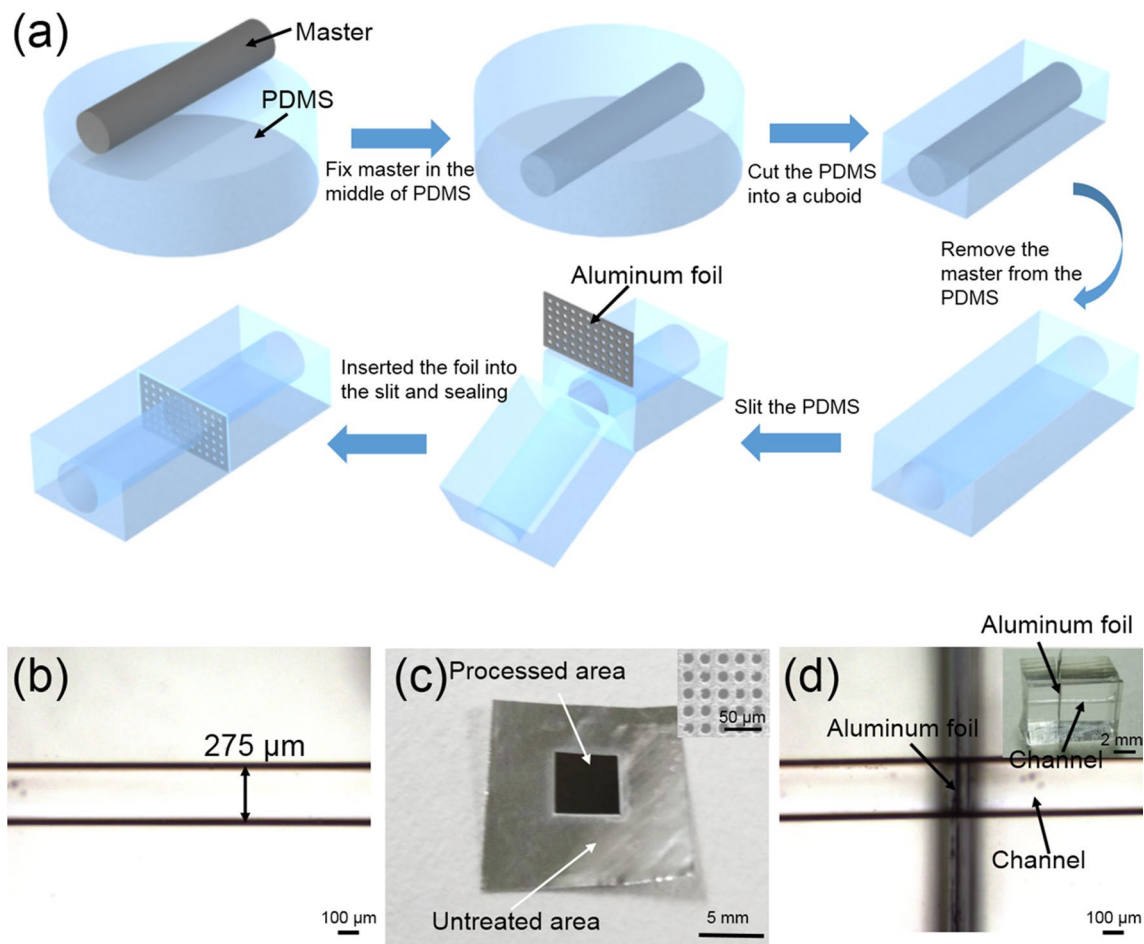


**Fig. 1** Novel fabrication scheme for the vertical-sieve 3D microfilter chip. **a** The schematic diagram of the fabrication process for a microchannel and microfilter chip. The aluminum foil was vertically inserted into the microchannel and sealed by a clamp with rapid integration and high reliability. **b** Optical image of the prepared microchannel (275  $\mu\text{m}$ ). **c** The photograph images of the pre-prepared

robust aluminum foil. The large area ( $4.8 \times 4.8 \text{ mm}^2$ ) of the foil can be fabricated within 30 min, which showed fast processing capability of femtosecond laser perforating technique. The inset is the SEM image of the micropore arrays in the aluminum foil. **d** The resulted integration chip (the inset photograph of the device)

off from the Petri dish and immersed in ethanol for 20 min to remove the master (stainless steel wire) easily. Then, the PDMS was cut into a cuboid ( $8 \times 5.5 \times 5.5 \text{ mm}^3$ ) by a scalpel. In order to insert the aluminum foil, a slit ( $\sim 7 \text{ mm}$  deep) was made by the scalpel, while the bottom of the microchip was still connected. The robust porous aluminum foil was inserted into the slit carefully. Finally, a clamp was used to hold both ends of the microchannel to seal the slit.

### 3 Results and discussion

#### 3.1 Novel strategy for integrating of aluminum foil with robust micropore arrays into microchip

A device-insertion and pressure sealing method (Fig. 1a) was presented to integrate robust porous aluminum foil into

a 275  $\mu\text{m}$ -diameter microchannel (Fig. 1b). Aluminum foil as a common material is widely used in industry, food, medicine, chemicals and other fields which is flexible and can be readily bent or wrapped around objects. The porous aluminum foil was realized by using point-by-point femtosecond laser perforating. The thickness and the whole area of the foil (Fig. 1c) were 25  $\mu\text{m}$  and  $15 \times 15 \text{ mm}^2$ , respectively. The black area ( $5 \times 5 \text{ mm}^2$ ) containing 26,000 holes with diameter of 11.5  $\mu\text{m}$  (The inset of Fig. 1c) was processed just in 20 min, which demonstrates the high efficiency and large-area fabrication capability. The integrated microfluidic chip was obtained by vertical inserting the porous aluminum foil into the microchannel, as shown in optical microscopic image (Fig. 1d) and the digital photograph (The inset in Fig. 1d). Compared with those methods which directly fabricate 3D filters in a channel, our direct insertion technique was simple and effective. In addition, the package of a

microchip by a clamp made it easy to integrate an aluminum foil into a channel without blocking caused by prepolymer bonding. The robust vertical-sieve 3D microchip can be reused for many times just by disassembly and ultrasonic cleaning when it is clogged by particles.

### 3.2 Filtering property of the vertical-sieve 3D microchip

In order to demonstrate the filtering property of the vertical-sieve 3D microchip with micropore aluminum foil, two kinds of SiO<sub>2</sub> particles (10 and 20 μm) mixture was used. The concentration of the particles was about 1000 beads mL<sup>-1</sup> with the mixture ratio (67:33 for diameters of 20 μm:10 μm). The interspace between two pores was 18 μm which can be arbitrarily adjusted by programmable design. The particle suspension was injected from one side of the channel by a syringe pump with a flow velocity of 2 mL/min, as shown

in the time-lapsed microscopic images (Fig. 2a, b). It can be clearly identified that the particles (diameter of 10 μm) smaller than the pores can pass through the aluminum foil easily (Fig. 2a), whereas the particles (20 μm) larger than the pores were all blocked in front of the aluminum foil (Fig. 2b). With the time lapsing, the bigger particles clogged the porous foil and the smaller particles also began to be blocked, which restrict the further separation of particles (Supplementary video). The clogging can be solved by back-flow with velocity of 1 mL/min (mild clogging) or disassembling the microchip and ultrasonic cleaning of the aluminum foil (heavy clogging). The microscope images of the particle suspension before and after filtering (Insets of Fig. 2c, d) also verified that the 20 μm particles were all filtered out by the aluminum foil. The statistical results also demonstrated that the particles larger than the pores were removed with 100% efficiency which is defined as the ratio of the fraction of particles desired to the total fraction of particles in the

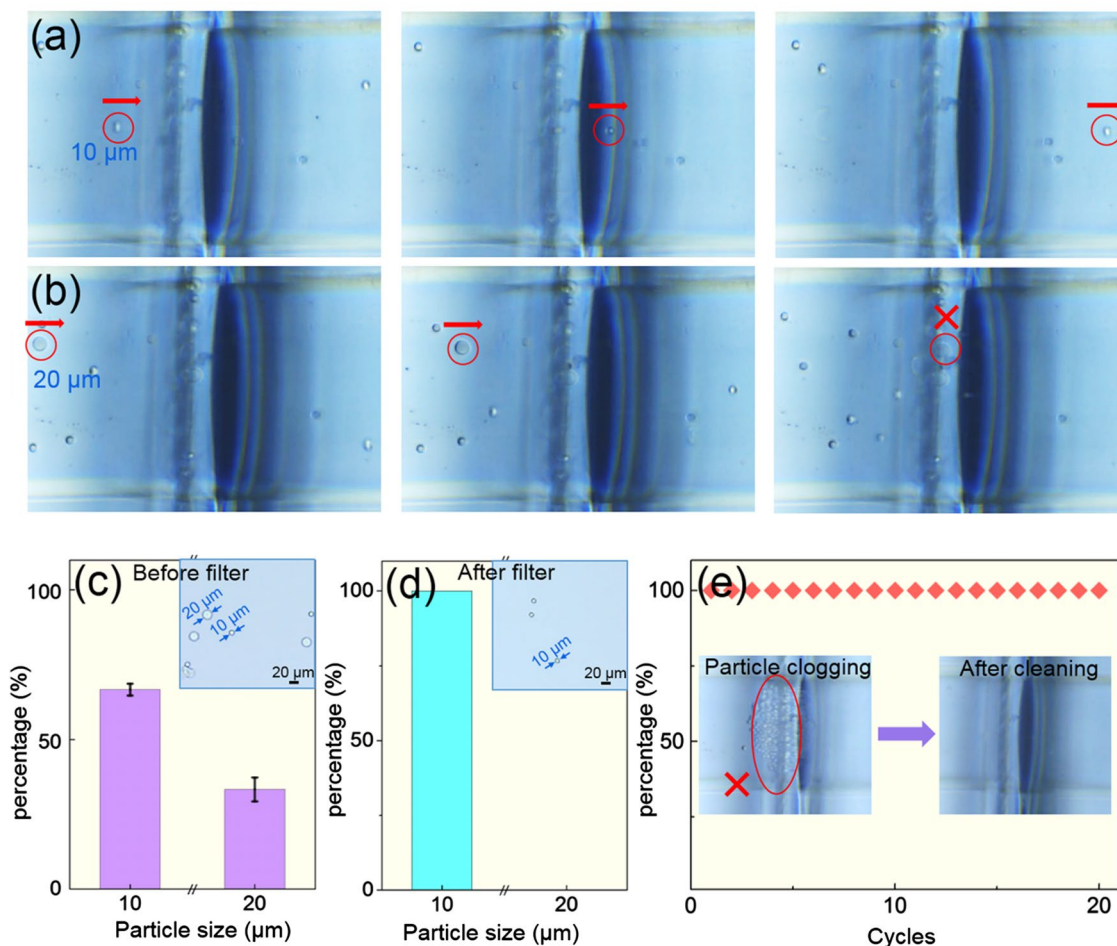


**Fig. 2** The filtering function (SiO<sub>2</sub> particles) of the vertical-sieve 3D microchip. **a** A 10-μm particle passing through the robust porous foil. **b** A 20-μm particle blocked by the aluminum foil. **c, d** The statistical results for different particles before and after filtering (the inset was

the optical images of the particle suspension before and after filtering). **e** The separation efficiency (100%) of the robust microchip after 20 times cycle cleaning (the inset is the optical image of the channel before and after cleaning)

outlet. After many times (~ 20 times) filtering and ultrasonic washing (Fig. 2e), the separation efficiency still kept 100% which proved the robustness and reusability of the porous aluminum foil.

### 3.3 Design and fabrication of the distinct sandwich-like microdevice for multisize filtering

To further demonstrate the versatility and flexibility of this novel device-insertion method, we designed a stacking multilayered structure (sandwich-like) microfluidic chip which can sort three different kinds of particles (20, 10 and 5 μm) and realize clogging-free separation with a high efficiency and large flux. As shown in Fig. 3a, the sandwich-like microchip consisted of five parts: two aluminum foils with different size of pores (7.8 and 11.5 μm), top flow layer (10 × 9×2 mm<sup>3</sup>), insulation (10 × 9×1 mm<sup>3</sup>) and bottom flow layers (10 × 9×2 mm<sup>3</sup>). Here, the same mold method was employed to fabricate the PDMS slabs. The

glasses (5 × 4×1 mm<sup>3</sup> for top flow layer and 8 × 4×1 mm<sup>3</sup> for insulation layer and bottom layer) as the masters were fixed in the bottom of a Petri dish, and the mixture of the curing agent and the PDMS prepolymer was spin-coated in the Petri with a spin rate of 300 rpm for controlling the thickness of the mixture (2 and 1 mm, respectively). After curing on a hotplate for 30 min, the PDMS slab was peeled from the Petri. The assembly process is illustrated in Fig. 3a. The porous aluminum foil (11.5 μm) was sandwiched between the top flow and insulation layer, which was used for filtering out particles with diameter of 20 μm from a mixed sample (20, 10 and 5 μm). The 7.8 μm porous aluminum foil was sandwiched between insulation and bottom flow layers which can remove particles with diameter of 10 μm and let the particles with diameter of 5 μm pass through. Finally, the sandwiched structure microchip was obtained, as shown in the digital photographs (Top view in Fig. 3d and side view Fig. 3e).

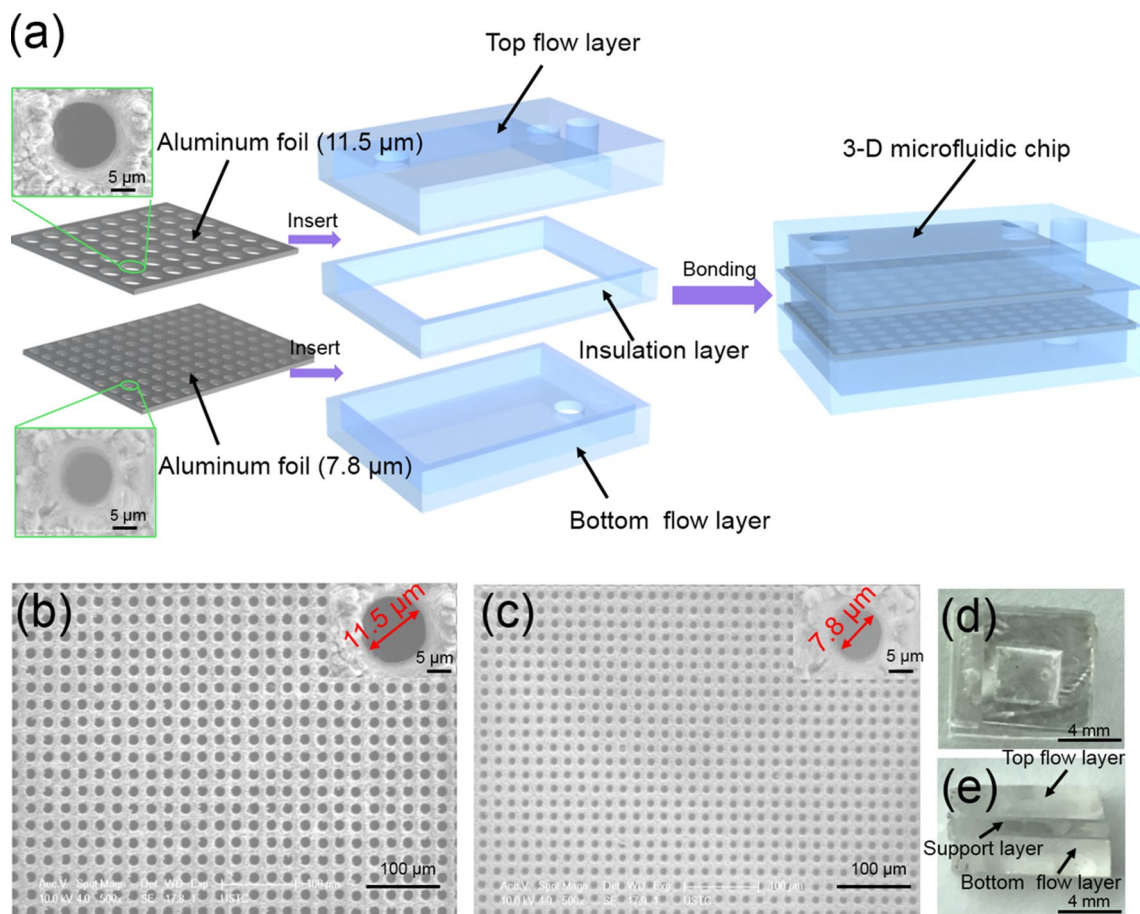


**Fig. 3** Processing scheme of the sandwich-like microchip for three kinds of different particles sorting with a high efficiency and large flux. **a** Schematic procedure for fabricating a 3D sandwich-like microchip. **b, c** SEM images of the multipores aluminum foils with

different diameters of 11.5 and 7.8 μm, respectively. The pores show uniform size and the interspace between two holes was 18 μm which can be tuned by arbitrarily adjusted by programmable design. **d, e** The photography of the sandwich-like 3D microfluidic chip

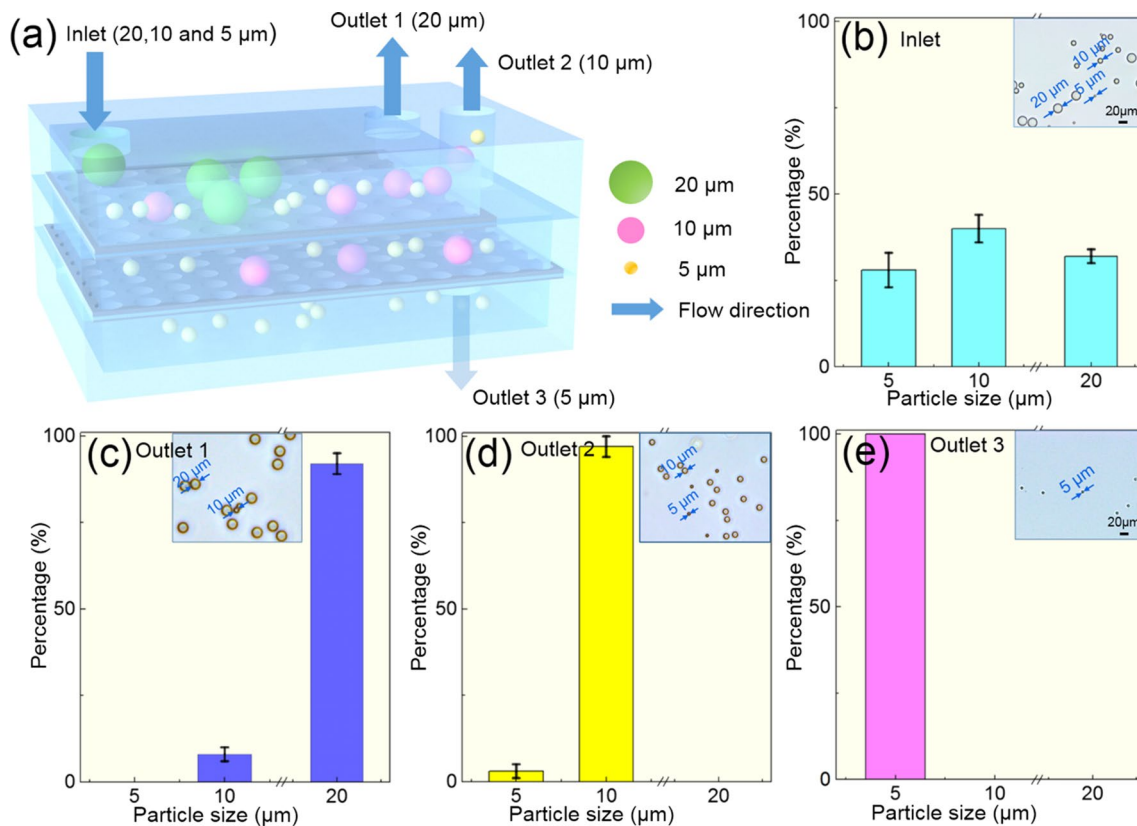


**Fig. 4** The sorting function of the sandwich-like microdevice. **a** Procedure for sorting particles with three kinds of different sizes (20, 10 and 5 μm). **b–e** The percentage of the SiO<sub>2</sub> particle mixture before and after filter (the inset is the optical images of particles in different stage). **c** The percentage of the microparticles from outlet 1 which

showed all 5 μm and most of 10 μm particles were removed. **d** 5 and 10 μm particles mixture in outlet 2 which showed the 20 μm particles were all filtered out by aluminum foil (11.5 μm). **e** Only 5 μm particles can be collected from outlet 3

Due to the excellent control of fs laser perforating, the fabricated porous aluminum foils present uniformly distributed micropore arrays (Fig. 3b, c). However, micro-nanostructures could be formed around the holes due to the resolidification of aluminum foil during femtosecond laser perforating (The inset images in Fig. 3b, c). It is well known that the ablation threshold fluence  $\phi(N)$  for  $N$  laser shots is related to the single-shot ablation threshold fluence by a power law:

$$\phi_{th}(N) = \phi_{th}(1)N^{S-1}$$

where the incubation coefficient  $S$  characterizes the extent to which incubation occurs in the material (Mannion et al. 2004). The lower energy and more pulse number (15 mW, 160) were used to fabricate the pores with 7.8 μm diameter, while the higher energy and less pulse number (30 mW, 100) were used for the fabrication of 11.5 μm-diameter pores. The smallest size of pore is about 3 μm due to the size of the laser focal spot (Supplementary Material).

### 3.4 Demonstration of the sorting property of the sandwich-like microchip

The silicon dioxide (SiO<sub>2</sub>) microspheres (with diameter of 20, 10 and 5 μm, respectively, the inset of Fig. 4b) suspended in the deionized water were used to characterize the efficiency of the sorter. The concentration of the microspheres was 1000 beads mL<sup>-1</sup> with the mixture ratio (40:32:28 for diameters of 20 μm:10 μm:5 μm). The separation procedure illustrated in Fig. 4a can be divided into two steps: filtering section and flushing section. First the particle suspension was injected into inlet by a syringe pump (SPLab01, Shenzhen, China) with 2 mL/min. When the mixture meets the top flow chamber, 20 μm particles were all filtered out by the first layer of aluminum foil. The 20 μm particles can be obtained from the outlet 1 with a high percentage (~92%, Fig. 4c) by subsequently flushing with deionized water while 10 and 5 μm particles passed through and flowed in the

insulation flow layer. The particles (10  $\mu\text{m}$ ) were extracted from outlet 2 (outlet 1 and 3 closed) (Fig. 4d) with a high percentage ( $\sim 97\%$ ). When the outlet 1 and 2 were closed, the particle suspension (10 and 5  $\mu\text{m}$ ) continued flowing from the insulation flow chamber to the bottom flow chamber, and the particles (10  $\mu\text{m}$ ) were trapped on the second foil while 5  $\mu\text{m}$  particles were collected at the outlet 3. The statistical results (Fig. 4e) indicated that 100% particles larger than pores had been successfully filtered out, which can be verified from the optical images of the particles (The insets). In separation process, some particles (10 and 5  $\mu\text{m}$ ) may stay on the first aluminum foil (11.8  $\mu\text{m}$ ), and 20  $\mu\text{m}$  particles mostly clogged on the pores which decreased the efficiency of the separation. This phenomenon can be avoided by reversing flow from outlet 3 to flush the microchip (outlet 1 and 2 closed) under mild clogging condition. With serious clogging, the porous aluminum foil in the microchip need to be disassembled to cleaned.

#### 4 Conclusion

This work presents a simple, rapid and effective way to fabricate the integrated microchip with filtering property by robust porous aluminum foil-insertion and pressure sealing techniques. The aluminum foil with large-area (10  $\times$  10  $\text{cm}^2$ ) porous arrays was fabricated by femtosecond laser perforating in a few minutes. The size and pattern of pores can be tuned from 3  $\mu\text{m}$  to several mm readily by adjusting the laser pulse energy and pulse number. Two different kinds of microfluidic chips were designed to demonstrate the feasibility of this device-insertion and pressure sealing method, which all realized the particles sorting with ultrahigh separation efficiency (92–100%). By disassembling the mechanical holder, the robust aluminum foil and microchip can be cleaned and reused for many times (more than 20 times). We believe this fast and effective approach for functional aluminum foil integration can offer a new possibility for LOC device design (Di Carlo et al. 2006), and will be widely applied in industry and biological fields.

#### References

- Aran K, Sasso LA, Kamdar N, Zahn JD (2010) Irreversible, direct bonding of nanoporous polymer membranes to PDMS or glass microdevices. *Lab Chip* 10:548–552. doi:10.1039/B924816A
- Bhagat AAS, Kuntaegowdanahalli SS, Papautsky I (2008) Enhanced particle filtration in straight microchannels using shear-modulated inertial migration. *Phys Fluids* 20:101702. doi:10.1063/1.2998844
- Dholakia K, Čižmár T (2011) Shaping the future of manipulation. *Nat Photonics* 5:335–342. doi:10.1038/nphoton.2011.80
- Di Carlo D, Wu LY, Lee LP (2006) Dynamic single cell culture array. *Lab Chip* 6:1445–1449. doi:10.1039/B605937F
- Jain A, Posner JD (2008) Particle dispersion and separation resolution of pinched flow fractionation. *Anal Chem* 80:1641–1648. doi:10.1021/ac0713813
- Jiang H-B, Zhang Y-L, Liu Y, Fu X-Y, Li Y-F, Liu Y-Q, Li C-H, Sun H-B (2016) Bioinspired few-layer graphene prepared by chemical vapor deposition on femtosecond laser-structured Cu foil. *Laser Photonics Rev* 10:441–450. doi:10.1002/lpor.201500256
- Kang JH, Park J-K (2007) Magnetophoretic continuous purification of single-walled carbon nanotubes from catalytic impurities in a microfluidic device. *Small* 3:1784–1791. doi:10.1002/sml.200700334
- Li G, Li J, Zhang C, Yanlei H, Li X, Chu J, Huang W, Dong W (2015a) Large-area one-step assembly of three-dimensional porous metal micro/nanocages by ethanol-assisted femtosecond laser irradiation for enhanced antireflection and hydrophobicity. *Appl Mater Interfaces* 7:383–390. doi:10.1021/am506291f
- Li G, Yang L, Peichao W, Zhang Z, Li J, Zhu W, Yanlei H, Dong W, Chu J (2015b) Fish scale inspired design of underwater superoleophobic microcone arrays by sucrose solution assisted femtosecond laser irradiation for multifunctional liquid manipulation. *J Mater Chem A* 3:18675–18683. doi:10.1039/C5TA05265C
- Liu Y, Lim K-M (2011) Particle separation in microfluidics using a switching ultrasonic field. *Lab Chip* 11:3167–3173. doi:10.1039/C1LC20481E
- Mannion PT, Magee J, Coyne E, O'Connor GM, Glynn TJ (2004) The effect of damage accumulation behaviour on ablation thresholds and damage morphology in ultrafast laser micromachining of common metals in air. *Appl Surf Sci* 233:275–287. doi:10.1016/j.apsusc.2004.03.229
- McCloskey KE, Chalmers JJ, Zborowski M (2003) Magnetic cell separation: characterization of magnetophoretic mobility. *Anal Chem* 75:6868–6874. doi:10.1021/ac034315j
- McGloin D (2006) Optical tweezers: 20 years on. *Philos Trans A Math Phys Eng Sci* 364:3521–3537. doi:10.1098/rsta.2006.1891
- Mohamed H, Turner JN, Caggana M (2007) Biochip for separating fetal cells from maternal circulation. *J Chromatogr A* 1162:187–192. doi:10.1016/j.chroma.2007.06.025
- Moorthy J, Beebe DJ (2003) In situ fabricated porous filters for microsystems. *Lab Chip* 3:62–66. doi:10.1039/B300450C
- Nam J, Lim H, Kim C, Yoon Kang J, Shin S (2012) Density-dependent separation of encapsulated cells in a microfluidic channel by using a standing surface acoustic wave. *Biomicrofluidics* 6:024120. doi:10.1063/1.4718719
- Nilsson A, Petersson F, Jönsson H, Laurell T (2004) Acoustic control of suspended particles in micro fluidic chips. *Lab Chip* 4:131–135. doi:10.1039/B313493H
- Park J-S, Jung H-I (2009) Multifurcated flow fractionation: continuous size-based separation of microspheres using a series of contraction/expansion microchannels. *Anal Chem* 81:8280–8288. doi:10.1021/ac9005765
- Sajeesh P, Sen AK (2014) Particle separation and sorting in microfluidic devices: a review. *Microfluid Nanofluidics* 17:1–52. doi:10.1007/s10404-013-1291-9
- Sethu P, Sin A, Toner M (2006) Microfluidic diffusive filter for apheresis (leukapheresis). *Lab Chip* 6:83–89. doi:10.1039/B512049
- Shi J, Mao X, Ahmed D, Colletti A, Huang TJ (2008) Focusing microparticles in a microfluidic channel with standing surface acoustic waves (SSAW). *Lab Chip* 8:221–223. doi:10.1039/B716321E
- Sugioka K, Cheng Y (2014) Ultrafast lasers—reliable tools for advanced materials processing. *Light Sci Appl* 3:e149t. doi:10.1038/lsa.2014.30
- Takagi J, Yamada M, Yasuda M, Seki M (2005) Continuous particle separation in a microchannel having asymmetrically arranged multiple branches. *Lab Chip* 5:778–784. doi:10.1039/B501885D

- Wang X (2005) Solidification and epitaxial regrowth in surface nanostructuring with laser-assisted scanning tunneling microscope. *J Appl Phys* 98:114304. doi:[10.1063/1.2135416](https://doi.org/10.1063/1.2135416)
- Weddemann A, Wittbracht F, Auge A, Hütten A (2009) A hydrodynamic switch: microfluidic separation system for magnetic beads. *Appl Phys Lett* 94:173501. doi:[10.1063/1.3123809](https://doi.org/10.1063/1.3123809)
- Wei H, Chueh B-H, Huiling W, Hall EW, Li C-W, Schirhagl R, Lin J-M, Zare RN (2011) Particle sorting using a porous membrane in a microfluidic device. *Lab Chip* 11:238–245. doi:[10.1039/C0LC00121J](https://doi.org/10.1039/C0LC00121J)
- Whitesides GM (2006) The origins and the future of microfluidics. *Nature* 442:368–373. doi:[10.1038/nature05058](https://doi.org/10.1038/nature05058)
- Wu D, Steckl AJ (2009) High speed nanofluidic protein accumulator. *Lab Chip* 9:1890–1896. doi:[10.1039/B823409D](https://doi.org/10.1039/B823409D)
- Xiao K, Grier DG (2010) Sorting colloidal particles into multiple channels with optical forces: prismatic optical fractionation. *Phys Rev E Stat Nonlin Soft Matter Phys* 82:051407. doi:[10.1103/PhysRevE.82.051407](https://doi.org/10.1103/PhysRevE.82.051407)
- Xiao Z, Wang A, Perumal J, Kim D-P (2010) Facile fabrication of monolithic 3D porous silica microstructures and a microfluidic system embedded with the microstructure. *Adv Funct Mater* 20:1473–1479. doi:[10.1002/adfm.200902164t](https://doi.org/10.1002/adfm.200902164t)
- Xu B, Du W-Q, Li J-W, Hu Y-L, Yang L, Zhang C-C, Li G-Q, Lao Z-X, Ni J-C, Chu J-R, Wu D, Liu S-L, Sugioka K (2016) High efficiency integration of three-dimensional functional microdevices inside a microfluidic chip by using femtosecond laser multifoci parallel microfabrication. *Sci Rep*. doi:[10.1038/srep19989](https://doi.org/10.1038/srep19989)
- Yamada M, Nakashima M, Seki M (2004) Pinched flow fractionation: continuous size separation of particles utilizing a laminar flow profile in a pinched microchannel. *Anal Chem* 76:5465–5471. doi:[10.1021/ac049863r](https://doi.org/10.1021/ac049863r)
- Yoon DH, Ha JB, Bahk YK, Arakawa T, Shoji S, Go JS (2009) Size-selective separation of micro beads by utilizing secondary flow in a curved rectangular microchannel. *Lab Chip* 9:87–90. doi:[10.1039/B809123D](https://doi.org/10.1039/B809123D)
- Zheng S, Lin H, Liu J-Q, Balic M, Datar R, Cote RJ, Tai Y-C (2007) Membrane microfilter device for selective capture, electrolysis and genomic analysis of human circulating tumor cells. *J Chromatogr A* 1162:154–161. doi:[10.1016/j.chroma.2007.05.064](https://doi.org/10.1016/j.chroma.2007.05.064)